JACS
JOURNAL OF THE AMERICAN CHEMICAL SOCIETY
Article
pubs.acs.org/JACS

Calcium Rubies: A Family of Red-Emitting Functionalizable Indicators Suitable for Two-Photon Ca^{2+} Imaging

Mayeul Collot,[†,‡,§] Christina Loukou,[†,‡,§] Aleksey V. Yakovlev,[◆,∥,⊥,○] Christian D. Wilms,[¶,□] Dongdong Li,[▽,#,△] Alexis Evrard,[▽,#,△] Alsu Zamaleeva,[◆,∥,⊥] Laurent Bourdieu,[◆,∥,⊥] Jean-François Léger,[◆,∥,⊥] Nicole Ropert,[▽,#,△] Jens Eilers,[¶] Martin Oheim,[▽,#,△] Anne Feltz,[◆,∥,⊥] and Jean-Maurice Mallet*[,†,‡,§]

[†]UPMC Université Paris 06, Ecole Normale Supérieure (ENS), Paris, F-75005 France
[‡]CNRS UMR 7203, Paris F-75005, France
[§]Laboratory of Biomolecules (LBM), Paris F-75005, France
[◆]Institut de Biologie (IBENS), Ecole Normale Supérieure (ENS), Paris F-75005, France
[∥] INSERM U1024, Paris F-75005, France
[⊥]CNRS UMR 8197, Paris F-75005, France
[¶]Carl-Ludwig-Institute for Physiology, Leipzig University, D-04103 Leipzig, Germany
[▽]INSERM U603, Paris F-75006, France
[#]CNRS UMR 8154, Paris F-75006, France
[△]Laboratory of Neurophysiology and New Microscopies, Université Paris Descartes, PRES Sorbonne Paris Cité, Paris F-75006, France

Supporting Information

ABSTRACT: We designed Calcium Rubies, a family of functionalizable BAPTA-based red-fluorescent calcium (Ca^{2+}) indicators as new tools for biological Ca^{2+} imaging. The specificity of this Ca^{2+}-indicator family is its side arm, attached on the ethylene glycol bridge that allows coupling the indicator to various groups while leaving open the possibility of aromatic substitutions on the BAPTA core for tuning the Ca^{2+}-binding affinity. Using this possibility we now synthesize and characterize three different CaRubies with affinities between 3 and 22 μM. Their long excitation and emission wavelengths (peaks at 586/604 nm) allow their use in otherwise challenging multicolor experiments, e.g., when combining Ca^{2+} uncaging or optogenetic stimulation with Ca^{2+} imaging in cells expressing fluorescent proteins. We illustrate this capacity by the detection of Ca^{2+} transients evoked by blue light in cultured astrocytes expressing CatCh, a light-sensitive Ca^{2+}-translocating channelrhodopsin linked to yellow fluorescent protein. Using time-correlated single-photon counting, we measured fluorescence lifetimes for all CaRubies and demonstrate a 10-fold increase in the average lifetime upon Ca^{2+} chelation. Since only the fluorescence quantum yield but not the absorbance of the CaRubies is Ca^{2+}-dependent, calibrated two-photon fluorescence excitation measurements of absolute Ca^{2+} concentrations are feasible.

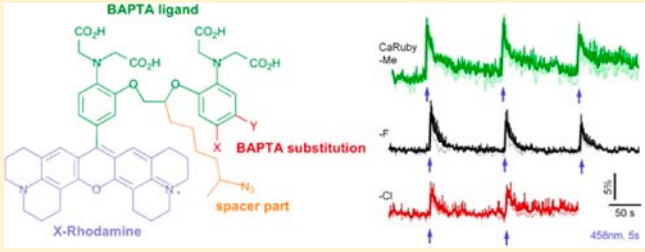

1. INTRODUCTION

Fluorescent Ca^{2+} indicators are indispensable tools for studying spatiotemporal fluctuations of intracellular free Ca^{2+} concentration ($[Ca^{2+}]_i$).[1,2] Ca^{2+} is an ubiquitous second messenger involved in numerous intracellular signaling cascades. Biological Ca^{2+} signals gain their specificity from operating at different temporal, spatial, and concentration scales. Temporally, Ca^{2+} transients cover the submillisecond to hour scale. Confined Ca^{2+} microdomains coexist with large-scale fluctuations which propagate through multicellular networks that extend over hundreds of micrometers. Cellular Ca^{2+} signals cover concentrations from near ~100 nM for the basal free $[Ca^{2+}]_i$ of most mammalian cells to >100 μM at the peak of Ca^{2+} microdomains. Thus, depending on the specific Ca^{2+} signal investigated, Ca^{2+} indicators with different affinity for Ca^{2+} binding ($K_{D,Ca}$) will be required as fluorescent reporters. Its fast on-rate for Ca^{2+} binding and high selectivity for Ca^{2+} over Mg^{2+} has made BAPTA[3] (1,2-bis(o-aminophenoxy)ethane-*N*,*N*,*N*′,*N*′-tetraacetic acid) the most popular Ca^{2+} chelator used in the synthesis of chemical Ca^{2+} indicators. A broad range

Received: May 20, 2012
Published: July 20, 2012

   dx.doi.org/10.1021/ja304018d | J. Am. Chem. Soc. 2012, 134, 14923−14931

of indicators has been synthesized by linking or integrating BAPTA to various chromophores.[4]

Most Ca^{2+} indicators, and certainly those that work best, combine BAPTA with fluorescein derivatives and hence emit yellow/green fluorescence.[5,6] However, the increasing use of cells transfected with fluorescent proteins (FPs),[5] of FP-expressing transgenic mice for targeting identified subpopulations of cells, together with the advent of optical techniques for purposes other than imaging require the development of new genetically encoded[2,7−9] and chemical Ca^{2+} probes.[2,10−12] Although monomeric red FPs are available, green or yellow FP tags are the most common. Introduced in 2012, GECO-R[13] is the only red-emitting genetically encoded Ca^{2+}-sensor whereas other FP-based Ca^{2+} indicators remain limited to green hue. The demand for longer-wavelength and higher signal-to-noise chemical Ca^{2+} indicators is accentuated by the recent trend toward all-optical manipulation and recording. Photopharmacology, photochemical uncaging, and optogenetics[14,15] all use near-ultraviolet or short visible wavelengths that further restrain the part of the visible spectrum available for Ca^{2+} imaging. Taken together, to be valuable for biological Ca^{2+} imaging, new Ca^{2+} probes should be bright, operate in spectral windows outside the yellow/green, and have a tunable $K_{D,Ca}$.

In this context, we introduced the red-emitting low-affinity ($K_{D,Ca} \sim 20\ \mu M$) indicator CaRuby-Cl,[16] a chloride-substituted BAPTA incorporated into an extended rhodamine (X-Rhodamine) having an extra side arm for conjugation to dextrans,[17] nanoparticle surfaces,[18] or other molecular targets. The attachment of the linker arm on the ethylene glycol bridge leaves us with the possibility for aromatic substitutions on the BAPTA (Scheme 1) that did not change the rhodamine spectrum (inset). We now systematically exploit these two properties to enlarge the CaRuby family and provide red-fluorescent indicators covering the micromolar range of affinities for Ca^{2+} binding ($K_{D,Ca}$).

Scheme 1. Generic Structure of the CaRubies

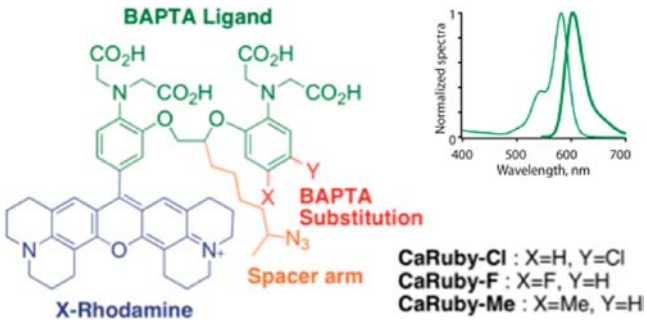

This paper is organized as follows. After their physicochemical characterization, we validate the chloride-, fluoride-, and methyl-substituted CaRubies for biological Ca^{2+} imaging by the detection of light-evoked near-membrane Ca^{2+} transients in cultured astrocytes expressing CatCh (calcium translocating channelrhodopsin), a Ca^{2+}-translocating channelrhodopsin, using total internal reflection fluorescence microscopy (TIRFM). We next characterize, using infrared fs-pulsed excitation, the utility of the CaRuby family for two-photon excitation fluorescence (2PEF) microscopy, both in the intensity- and fluorescence-lifetime domain. Fluorescence lifetimes of the Ca^{2+}-free and -bound forms of all three dyes are reported, allowing calibrated $[Ca^{2+}]_i$ measurements with 2PEF time-correlated single-photon counting (TCSPC).[19]

2. RESULTS AND DISCUSSION

The three fluorescent Ca^{2+} indicators described in this article consist of a BAPTA Ca^{2+}-chelating moiety with a -Cl, -F, or Me-substituted on one of the aromatic rings. The functionalizable azido side arm is introduced at an early stage of the synthesis whereas the X-rhodamine is synthesized thereafter, leading to the functional Ca^{2+} indicator, which we refer to as CaRuby-Cl, -F, or -Me depending on the substitution. The detailed synthesis of these molecules is reported in the Supporting Information.

In a solution containing 100 mM KCl, 30 mM MOPS (3-(*N*-morpholino)propanesulfonic acid), and 10 mM NTA (nitrilotriacetic acid) (at pH 7.2), CaRuby-Cl, -F. or -Me had apparent $K_{D,Ca}$s of 3, 6, and 22 μM (Figure 1a and Table 1). For all probes fluorimetric titration curves indicated a 1:1 Ca^{2+} binding, suggesting that the presence of the linker arm does not modify the stoichiometry of Ca^{2+} binding. All three CaRubies had absorbance and fluorescence peaks near 586 and 604 nm, respectively (Scheme 1, inset), and fluorescence quantum yields φ were around 0.55 when bound to Ca^{2+} (Table 1 and Figure S1 of the Supporting Information). CaRubies were virtually nonfluorescent in a nominally Ca^{2+}-free solution containing 10 mM ethylene glycol tetraacetic acid (EGTA). Relative peak fluorescence (dF/F_0, measured at 604 nm) increased more than 50-fold upon Ca^{2+} binding and resulted from a Ca^{2+}-dependent change in φ, rather than absorbance.[16]

Ca^{2+} indicators are exposed to ionic conditions that potentially interfere with Ca^{2+} chelation. In the cytoplasm, Mg^{2+} is the most prevalent divalent cation. We therefore first measured CaRuby fluorescence in a pH- and Ca^{2+}-buffered solution containing 50 μM free Mg^{2+} and 50 μM free Ca^{2+} (free ion concentrations in the presence of pH and Ca^{2+} buffers were calculated as described in the Supporting Information of ref 16) and found no difference to the fluorescence measured in 50 μM free Ca^{2+} alone (Figure 1b).

For testing how the presence of other divalent cations affected the fluorescence, we established a fluorescence baseline with copper quenching[20] and used an ion-displacement assay: CaRuby-Me was strongly fluorescent in solutions containing 50 μM Ca^{2+}, Ba^{2+}, or Cd^{2+}, whereas the paramagnetic transition metal ions (Co^{2+}, Cu^{2+}, Ni^{2+}) acted as quenchers. Adding 50 μM Ca^{2+} to these solutions did not measurably alter CaRuby-Me fluorescence, suggesting that Ca^{2+} was unable to displace already complexed Co^{2+}, Cu^{2+}, Mn^{2+}, Ni^{2+}, or Zn^{2+} (Figure 1c). The corresponding and similar data for CaRuby-F are shown in Figure S2 of the Supporting Information. Finally, we investigated the pH-dependence of CaRuby fluorescence and found intensity changes below 20% over the physiologically relevant range from 6.8 to 7.6, with a pK_a around 6.2 for all three CaRubies (Figure 1d). Taken together, our new Ca^{2+} indicators combine the spectral properties of an X-rhodamine with the high selectivity for Ca^{2+} over Mg^{2+} and low pH sensitivity of a BAPTA-based indicator.[3]

The major asset of our CaRubies over existing rhodamine-based Ca^{2+} probes[21] is the combination of their tunable affinity for Ca^{2+} binding and the functionalizable azido arm. The azido group enables different kinds of coupling reactions (Figure 2). We illustrate this capacity by coupling an alkyne or active ester via the Huisgen 1,3-dipolar cycloaddition (click chemistry) or

dx.doi.org/10.1021/ja304018d | J. Am. Chem. Soc. 2012, 134, 14923−14931

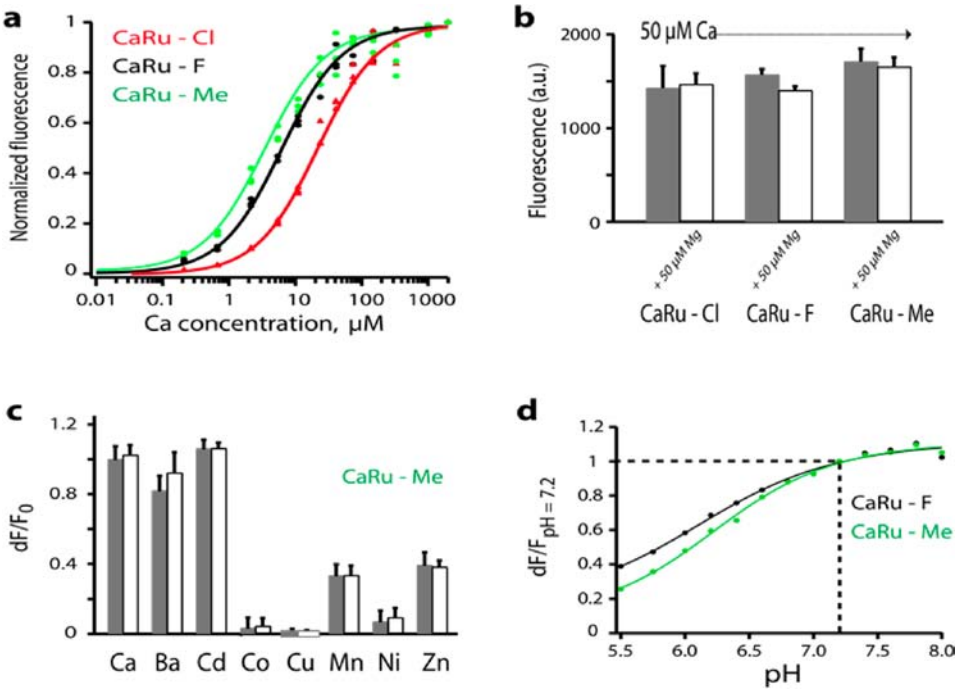

Figure 1. Physico-chemical characterization of CaRubies. (a) Fluorimetric titration against Ca^{2+} in a buffer containing (in mM) 100 KCl and 30 MOPS (pH 7.2). Lines are Hill fits with all data points from three independent titrations for each dye. See Table 1 for $K_{D,Ca}$ values. (b) Fluorescence of CaRuby-Cl, -F, and -Me, in the presence of 50 μM free Ca^{2+} alone, gray, and in the presence of 50 μM free Ca^{2+} and 50 μM free Mg^{2+}, white. (c) Normalized fluorescence of CaRuby-Me (relative to that in the presence of 50 μM free Ca^{2+}) in solutions containing 50 μM of either Ca^{2+}, Ba^{2+}, Cd^{2+}, Co^{2+}, Cu^{2+}, Mn^{2+}, Ni^{2+}, or Zn^{2+}, gray, and upon addition of 50 μM Ca^{2+}, white. (d) pH dependence of of CaRuby-Me and -F fluorescence in a buffer containing (in mM) 100 KCl, 30 MOPS, 10 NTA, and 0.024 free Ca^{2+}. pK_a values from Hill fits were 6.27 ± 0.06 and 6.18 ± 0.14, respectively. In the physiologically relevant range between pH 6.8 and 7.6, fluorescence varied from 0.87 to 1.05 (unity at pH 7.2). Symbols and through lines show mean ±1 SD from three independent titrations and fit.

Table 1. Physicochemical Properties of the CaRuby Dyes[a]

CaRuby	$K_{D,Ca}$ (μM)	dF/F_0	φ_{CaF}	φ_{CaB}	pK_a
-Me	3.4 ± 0.47	62.5 ± 5.2	0.004 ± 0.02	0.58 ± 0.06	6.27 ± 0.06
-F	6.2 ± 1.03	49.7 ± 5.8	0.007 ± 0.02	0.57 ± 0.05	6.18 ± 0.14
-Cl	21.6 ± 2.7	51.9 ± 1.4	0.007 ± 0.02	0.55 ± 0.05	6.22 ± 0.07

[a]Mean ± 1 SD values; n = 3 independent titrations; φ: quantum yield in Ca free and 2 mM Ca^{2+} (CaF; CaB); others, see text).

the reduction of the azido group, respectively. These reactions were very efficient and are suitable for biological conjugation reactions. As an example, we linked CaRuby-Me with up to 76% yield to different molecular-weight poly(ethylene glycols) (PEGs). Conjugation had no adverse effect on Ca^{2+} chelation nor on the dynamic range for Ca^{2+} sensing (Figure S3, Supporting Information). Compared to their arm-free analogues, X-rhod-5F and X-rhod-1 (Figure S4, Supporting Information) CaRubies display a 3- to 4-times higher Kd,Ca presumably due to a restricted ethylene glycol C−C bond free rotation. However, their unique linker arm should make our CaRubies a versatile building block for subcellularly targeted Ca^{2+}probes, allowing their coupling to antibodies and bio-orthogonal tags or linking it to dextrans, nanoparticles, latex beads, or other substrates.[17,18,22]

Fluorescent Ca^{2+} indicators are commonly prepared as membrane impermeant salts for cytoplasmic loading by infusion from a patch pipette or as membrane-permeable esters that allow the simultaneous bulk loading of hundreds of cells.[1] We found earlier that CaRuby-Cl with a molecular weight of ∼1000 Da and a size of ∼1.5 nm was membrane-impermeable when applied to chromaffin cells, neurons, HEK293, or BON cells in culture, even when present overnight in the extracellular fluid.[17] A notable exception were cultured mouse cortical astrocytes that readily internalized the acid forms of all three CaRuby dyes following short incubations at room temperature (5 μM, 10 min, 20−22 °C). We observed a similar spontaneous uptake into astrocyte cultures with the structurally related rhodamines sulforhodamine 101 (SR101), R101, and SR-B. Depending on the dye, the subcellular distribution differed (Figure S5, Supporting Information). The mechanism of this astrocyte-specific uptake and compartmentalization is unknown but could result from a combined effect of charge and partitioning into lipids,[23,24] or the presence of an astrocyte-specific permeation or transport pathway.

In astrocytes expressing a light-gated Ca^{2+}-translocating channelrhodopsin coupled to yellow FP (CatCh-YFP)[25,26] and labeled with CaRuby-Me (Figure 3a), short flashes of blue light (458-nm, 5s, 13.6 mW/mm^2) elicited robust and reproducible near-membrane Ca^{2+} transients detectable with TIRFM (Figure 3b). The peak dF/F_0 values observed in response to this stereotyped light-evoked Ca^{2+} influx scaled in an affinity-dependent manner, following the sequence -Me > -F > -Cl (Figure 3c). The amplitude and time-course of light-

dx.doi.org/10.1021/ja304018d | J. Am. Chem. Soc. 2012, 134, 14923−14931

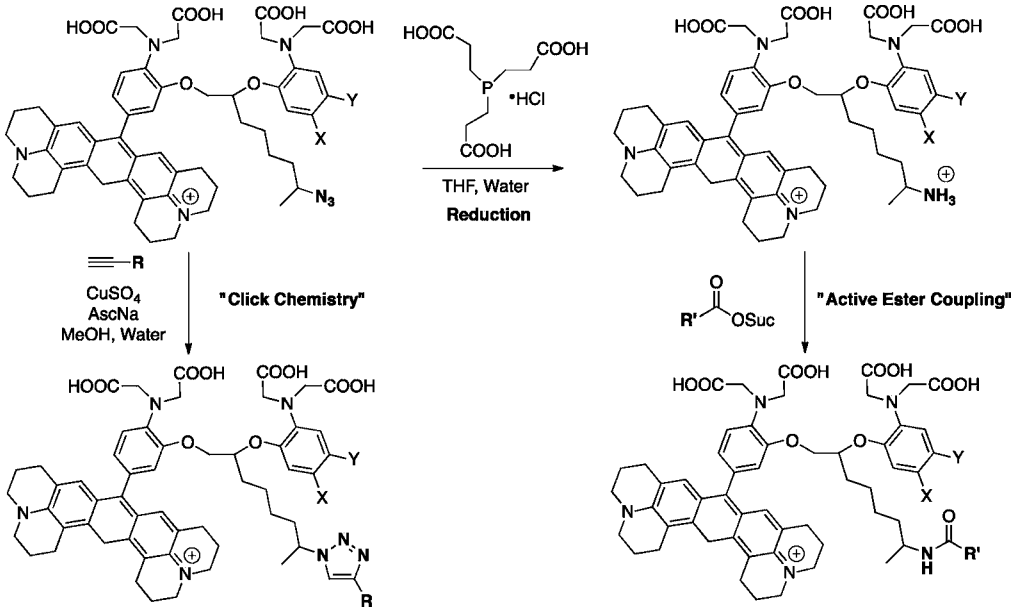

Figure 2. Coupling reactions involving CaRubies: click chemistry and amine-acid coupling (Asc: ascorbate; Suc: succinimide).

evoked Ca^{2+} transients could be further shaped by varying the duration of the light pulse (Figure 3d). Astrocytes responded to local ATP application (300 μM) with fast, spatially confined and high-amplitude Ca^{2+} transients detected with CaRuby-Me (dF/F_0 = 13.4 ± 4.6%; mean fwhm of 84.9 ± 40.2 ms; n = 24 events from N = 4 cells; Figure 3e) that were occluded by the global, homogeneous fluorescence increase seen in parallel experiments with the green-fluorescent high-affinity Ca^{2+} indicator Fluo-4, AM ($K_{D,Ca}$ 345 nM). In response to the same stimulus, the later reported slower and lasting Ca^{2+} transients having a mean amplitude of 49.7 ± 7.5% and fwhm of 11.8 ± 3.8 s (19 ROIs from 4 cells; Figure 3f).

The sulfonated X-rhodamines SR101/TexasRed are known to display a cell-type specific tropism for astrocytes when applied extracellularly to brain slices or as a drop on the cortical surface of the intact brain after craniotomy.[27,28] Similar results have been obtained after i.v. injection of different rhodamines.[29] In view of their spontaneous internalization into cultured astrocytes, we therefore tested whether CaRubies selectively labeled cortical astrocytes in situ. However, incubation (1 μM, 15 min) of acute brain slices from adult Aldhl1L1-EGFP mice that express EGFP under the control of an astrocyte-specific promoter revealed no astrocytic tropism of any of the three CaRubies whereas parallel experiments using SR101 confirmed the well-described astrocytic staining. Only at the surface of the brain slices was observed some sporadic labeling, suggesting a nonspecific uptake into cells damaged during the slicing procedure (Figure 4). Whether this difference between rhodamines concerning their astrocytic uptake is due to the bigger size of the CaRubies or resulting from a molecular recognition of the sulfonated X-rhodamines is beyond the scope of this paper.

Their long emission wavelengths make our CaRubies attractive probes for Ca^{2+} imaging in scattering media using two-photon excitation fluorescence (2PEF) detection. To determine the optimal excitation wavelength, we scanned the entire tuning range of the Ti:Sapphire laser. Femtosecond- (fs-) pulsed excitation in the 750 to 1000 nm range revealed 2PEF excitation peaks near 915 nm for all three CaRubies (inset in Figure 5) which is close to those of enhanced cyan fluorescent protein (ECFP) (860 nm),[30] EGFP (920–960 nm),[30–32] EYFP (950 nm),[30,32] and channelrhodopsin (920 nm).[33,34] In vivo, 20 min after a topical application of CaRuby-Me (10 μL, 100 μM) in a small cranial window above the rat cortex, we observed a perivascular labeling using 2PEF excitation at 900 nm (Figure 5). Perivascular staining has been reported recently for the structurally unrelated fluorophore AlexaFluor 633.[35]

Estimating absolute $[Ca^{2+}]_i$ levels from fluorimetric 2PEF measurements is made difficult by unknown dye concentrations and the attenuation of both the excitation power and 2PEF collection efficiency[36] with imaging depth. Pseudoratios with a second Ca^{2+}-insensitive reference dye[37,38] correct for some distortions but do not give access to absolute $[Ca^{2+}]_i$ levels. Advantageously, fs-pulsed excitation lends itself in a natural way to fluorescence lifetime measurements provided the decays for the Ca^{2+}-bound and free forms of the indicator are measurably different.[19] In Ca^{2+}-buffered solutions containing between 1 nM and 100 μM free Ca^{2+}, CaRuby-Me displayed a double-exponential fluorescence decay that was Ca^{2+}-dependent (Figure 6a). The amplitudes α of the fractional decay components were used to derive the amount of Ca^{2+}-free and -bound dye, respectively (Figure 6b). The $K_{D,Ca}$ and a correction factor S (see ref 19) were obtained by fitting the Hill equation with the normalized pre-exponential coefficients of the fast and slow decay components and were in good agreement with the $K_{D,Ca}$ values obtained from steady-state fluorescence measurements, Table 2. Taken together, their steady-state and time-resolved fluorescence properties make CaRuby dyes excellent candidates for quantitative 2PEF imaging of $[Ca^{2+}]_i$ in intact preparations.

3. CONCLUSION

We have enlarged the CaRuby family to provide three functionalizable red-emitting medium- to low-affinity Ca^{2+} indicators with physicochemical properties making them useful in a wide array of multicolor biological applications. The common and defining feature of our CaRubies is the linker arm allowing diverse couplings of the dyes. Unlike a linker anchored

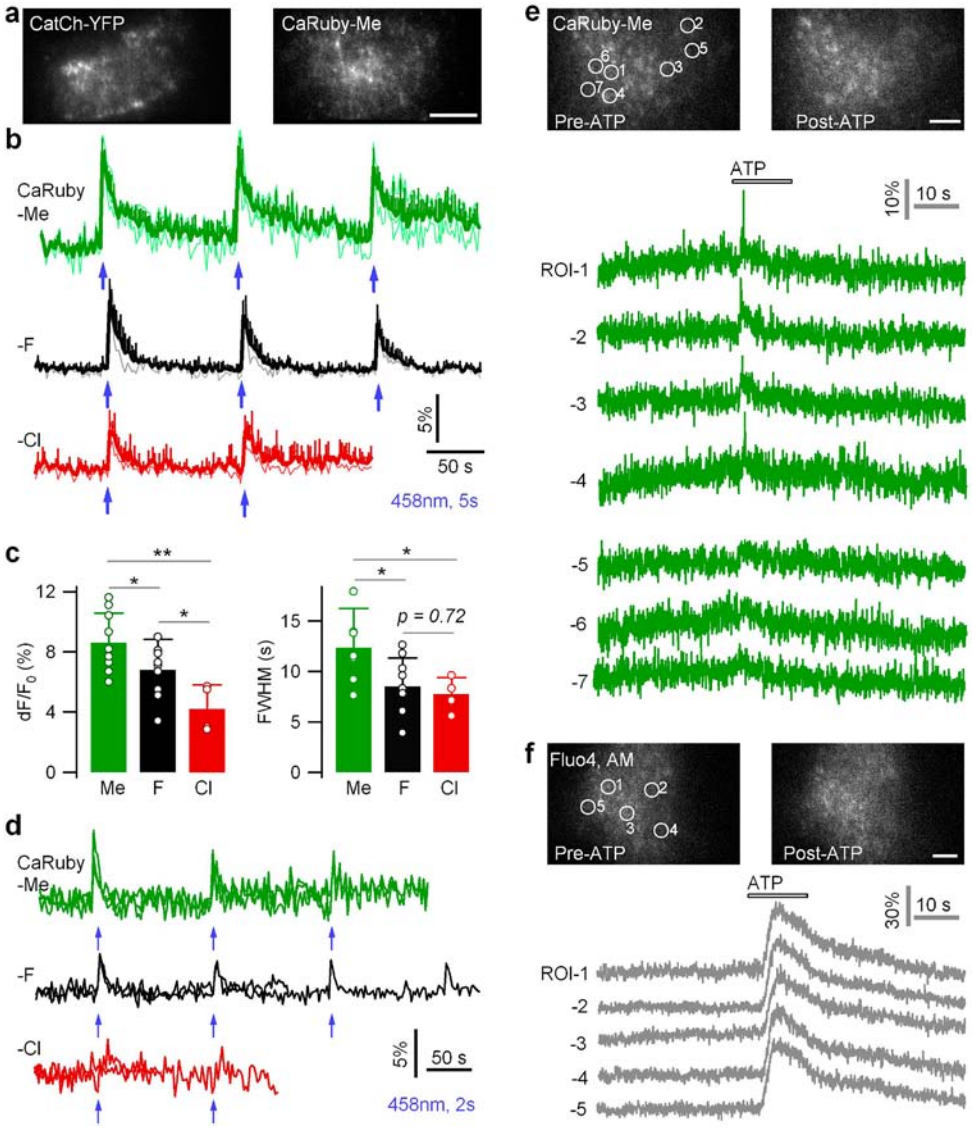

Figure 3. Multiband Ca^{2+} imaging and optogenetic stimulation with CaRuby. (a) Dual-color excitation (488/568 nm) and dual-color emission TIRFM images of an astrocyte expressing the light-gated Ca^{2+}-translocating CatCh-YFP (yellow fluorescent protein) loaded with CaRuby-Me (5 μM, 10 min). Scale bar, 10 μm. (b) CaRuby-Me, -F, and -Cl were used to monitor light-evoked Ca^{2+} rises (458 nm, 5 s, 13.6 mW/mm^2). Thin light traces show individual astrocytes, thick darker lines are population mean +1SD. (n = 9 trials in N = 3 cells for CaRuby-Me and -F, 4 trials in 2 cells for CaRuby-Cl). (c) Comparison of the peak amplitude (dF/F_0 = 8.7 ± 2.0%, 6.7 ± 1.7%, and 4.3 ± 1.6% for CaRuby-Me, -F, and -Cl, respectively) and the duration (full width at half-maximum, fwhm) of the Ca^{2+} responses scaled as expected from the lower Ca^{2+} affinity of CaRuby-Cl ($K_{D,Ca}$, 21.6 μM) compared to CaRuby-Me ($K_{D,Ca}$, 3.4 μM) and CaRuby-F ($K_{D,Ca}$, 6.2 μM). *, $p < 0.05$; **, $p < 0.01$. (d) In comparison with the responses evoked with 5 s light pulses, CaRuby-Me and CaRuby-Cl reported significantly lower Ca^{2+} rises with 2 s light pulses (5.1 ± 1.3%, 8 trials in 3 cells vs 8.7 ± 2.0%, 9 trials in 3 cells; 4.0 ± 0.6%, 6 trials in 2 cells vs 6.7 ± 1.7%, 9 trials in 3 cells, respectively; $p < 0.01$). Each trace represents the stimulation of a single astrocyte. (e) Local application of 300 μM ATP (adenosine triphosphate) from a puff pipet results in spatially confined Ca^{2+} transients in astrocytes detected with CaRuby-Me. Top panels show TIRFM images of an astrocyte acquired before and after stimulation. Circles identify seven regions of interest (ROIs, 2 μm diameter). Green traces show the evolution with time (imaged at 20 Hz) of dF/F_0 responses in the ROIs identified by number. Scale bar, 5 μm. (f) Same experiment with the high-affinity green-fluorescent Ca^{2+} indicator Fluo-4, AM that reported a homogeneous elevation throughout the entire astrocyte with no detectable Ca^{2+} microdomains. White circles identify five ROIs with the corresponding fluorescence responses shown as gray traces.

to the BAPTA aromatic ring,[22] its localization on the ethylene glycol bridge permits aromatic substitutions and hence a fine-tuning of the $K_{D,Ca}$.

With their long-wavelength emission and nonlinear excitation properties compatible with popular FPs, our CaRubies are excellent probes for Ca^{2+} imaging in otherwise challenging experiments relying on several excitation or emission bands. The combined light-stimulation and Ca^{2+}-imaging experiments using CatCh-YFP expressing cells validate the new indicators in such experiments that put strong constraints on the available wavelength windows.

Compared with the red-emitting bioluminescence resonance energy transfer (BRET)-based tandem-dimer tomato-aequorin[9] or the genetically encoded red-emitting Ca^{2+}-probe R-GECO,[13] the CaRubies build on the large and established toolbox of organic synthesis and can be prepared in a variety of different forms, as salts, as membrane-permeable esters, be attached to

dx.doi.org/10.1021/ja304018d | J. Am. Chem. Soc. 2012, 134, 14923−14931

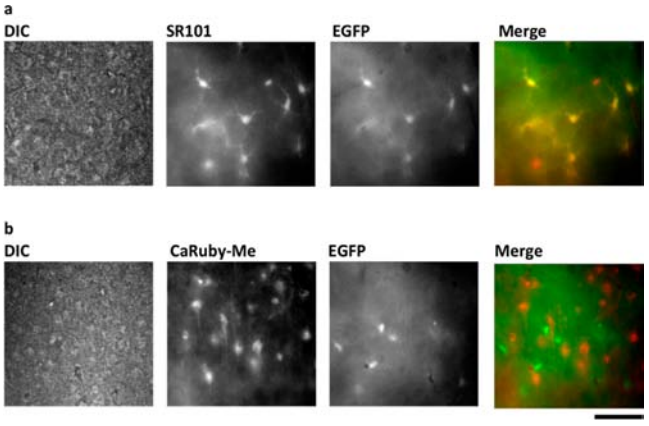

Figure 4. Comparison of sulforhodamine 101 (SR101) and CaRuby-Me labeling in acute coronal slices of adult transgenic Aldh1L1-EGFP mice. (a) Example of infrared (>900 nm) differential-interference contrast (DIC) and 488/568-nm dual-color epifluorescence raw images of cortical astrocytes loaded with SR101 (1 μM, 15 min) and expressing enhanced green fluorescent protein (EGFP) under the control of the astrocytic-specific marker Aldh1L1 (aldehyde dehydrogenase 1 family, member L1).[39] The pseudocolor overlay (merge) reveals a significant overlap between SR101 and EGFP fluorescence (yellow) as expected from earlier studies.[27−29] Similar results were obtained in the hippocampus (n = 3 slices of N = 2 animals, data not shown). (b) DIC, CaRuby-Me-, and EGFP-fluorescence images revealed distinct distributions of EGFP and spontaneously internalized CaRuby-Me in the cortex of Aldh1L1 transgenic mice. Similar nonoverlapping distributions were observed in various regions of n = 5 slices from N = 3 mice (not shown). The uptake of CaRuby-Me was prominent near the slice surface, suggesting that the dye might accumulate in cells damaged during slicing. Scale bar, 100 μm for all panels. Note the absence of cross-excitation and fluorescence bleed-though, respectively, allowing the simultaneous imaging of EGFP and CaRuby fluorescence.

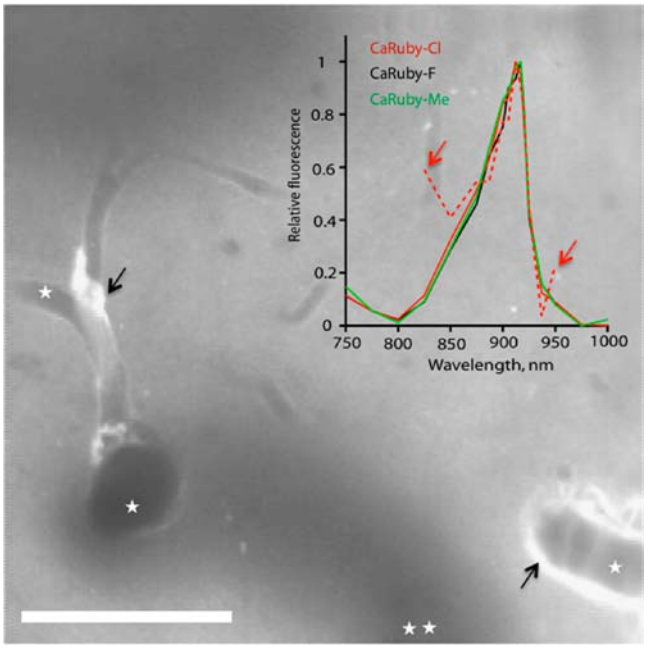

Figure 5. Two-photon excitation at 900 nm of CaRuby-Me at ~70 μm depth in the cortex of an anesthetized 3 months rat in vivo, 20 min after topical application of CaRuby-Me revealed perivascular labeling (white arrows). Blood vessels remained unstained (white stars). A deeper, large vessel (2 stars) is seen as a shadow. Scale bar, 50 μm. Inset: Normalized 2PEF spectra of CaRuby-Me (green), CaRuby-F (black), and CaRuby-Cl (red) bound to Ca^{2+} 2 mM (solid) and, for CaRuby-Cl, in nominally Ca^{2+}-free solution containing 5 mM EGTA (dashed). Spectra show a peak of 912 nm for CaRuby-Cl and 917 nm for CaRuby-F and -Me, respectively. For the less fluorescent Ca^{2+}-free (apo-) form of the dye (dashed) the higher excitation intensity required introduced a contamination at the edges of the scanned region (black arrows). No peak shift was detected upon Ca^{2+} binding.

large MW dextrans, or linked to specific bio-orthogonal tags permitting their subcellular targeting.[22]

4. EXPERIMENTAL SECTION

For general analytical procedures and synthetic protocols used to prepare the CaRubies and their PEGylated derivatives, please see the Supporting Information.

4.1. Reagents and Materials. *4.1.1. Chemicals.* The following chemicals were utilized in this investigation: 1 M $CaCl_2$ (Fluka 21115); DMEM (Invitrogen 31885); ethanol (Merck cat. no. 100983); Fluo-4, AM (Invitrogen cat. no. F-14201); 4-(2-hydroxyethyl)-1-piperazineethanesulfonic acid (HEPES) (Sigma-Aldrich; cat. no. H3375); KCl (Prolabo cat. no. 215GC); lipofectamine 2000 (Invitrogen; cat. no. 11668-027); methanol (Merck cat. no. 106009); MOPS (Sigma-Aldrich cat. no. M-1254); NTA (Sigma-Aldrich cat. no. N-9877); rhodamine 101 (Sigma-Aldrich; cat. no. 83694); sulforhodamine 101 (Sigma-Aldrich cat. no. S-7635); sulforhodamine-B (Sigma-Aldrich; cat. no. R6626); water (Fluka cat. no. 95305); X-rhod-1, AM (Invitrogen cat. no. X-14219).

4.1.2. Cells. Experiments followed the European Union and institutional guidelines for the care and use of laboratory animals (Council directive 86/609EEC). Cortical astrocytes were prepared from P0-1 (P0 being the day of birth) NMRI mice (Janvier , St Genest sur Ile, Mayenne, France) as previously described.[40,41] Briefly, the neocortex was dissected and mechanically dissociated. Cells were plated and maintained in Petri dishes for one week to reach confluence before their transfer onto coverslips (#1.5, BK-7, 25 mm diameter, Marienfeld Superior, Menzel ThermoFisher, Braunschweig, Germany). Secondary cultures were maintained in Dulbecco's modified Eagle's medium (DMEM) supplemented with 5% fetal bovine serum, penicillin (5 U/mL), and streptomycin (5 μg/mL) at 37 °C in a humidified 5% CO_2 atmosphere. Astrocytes kept for one more week in secondary culture and transfected with CatCh-YFP (see below) were incubated with CaRuby-Me, -F, or -Cl salt (5 μM, 10 min) at room temperature (RT, 20−22 °C) and perfused 30 min in dye-free medium to allow for complete wash-off of membrane-bound CaRuby-Me. During experiments, cells were continuously perfused at 0.5−1 mL/min with extracellular saline containing (in mM): 140 NaCl, 5.5 KCl, 1.8 $CaCl_2$, 1 $MgCl_2$, 20 glucose, 10 HEPES (pH 7.3, adjusted with NaOH).

4.1.3. Plasmids. Cultured astrocytes were transfected with CatCh-YFP[25] using lipofectamine 2000 and following standard protocols. We used 1.4 μg DNA plasmid for each coverslip. Cells were maintained in culture for 1−2 days after transfection to allow the expression and proper targeting of CatCh to the cell surface, detectable by TIRF imaging (see below) of the near-membrane space.

4.2. CaRuby Uptake in Acute Brain Slices. Adult Tg(Fthfd-EGFP)1 Gsat/Mmcd) mice expressing EGFP under the control of formyltetrahydrofolate dehydrogenase (Aldh1L1 or Fthfd)[42] were obtained from the Mutant Mouse Regional Resource Centers (MMRRC), Jackson Laboratory (Bar Harbor, MN), and backcrossed on an NMRI background. Mice were anesthetized by intraperitoneal injection of pentobarbital (20 mg/kg) and decapitated. Their brains were quickly removed and placed in ice-cold (2−4 °C) oxygenated (5% O_2, 95% CO_2) standard artificial cerebrospinal fluid (ACSF) containing, in mM: 126 NaCl, 2.85 KCl, 1.25 KH_2PO_4, 1.5 $MgSO_4$, 2 $CaCl_2$, 26 $NaHCO_3$, 5 sodium pyruvate, and 10 glucose. Coronal slices (400 μm thick) were cut on a vibratome (VT1000S, Leica, Wetzlar, Germany) and first maintained during 1 h at 33 °C for recovery, then at RT in oxygenated ACSF. Subsequently, slices were either incubated

dx.doi.org/10.1021/ja304018d | J. Am. Chem. Soc. 2012, 134, 14923−14931

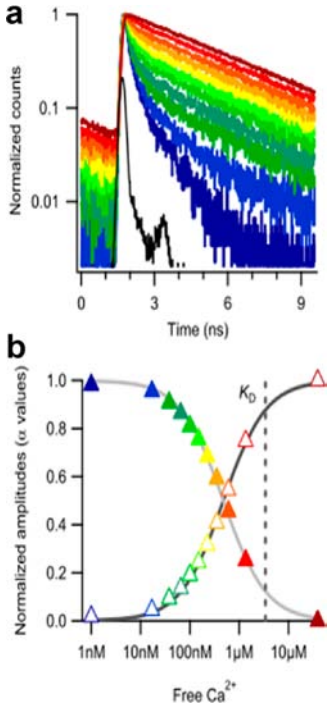

Figure 6. (a) Normalized 2PEF lifetimes of CaRuby-Me at different [Ca^{2+}] between 1 nM and 100 μM, color-coded as in part b; the black trace is the instrument response function. (b) Normalized amplitudes of the pre-exponential coefficients α of the fast and slow decay components (closed and open triangles, respectively) of a double-exponential global reconvolution fit to the data shown in part a. Solid lines are fits with the α_f and α_s values, yielding a $K_{D,Ca}$ of 3.4 ± 0.3 μM (dashed vertical line) indistinguishable from that obtained by steady-state fluorimetric titration (3.4 ± 0.47 μM). See Table 2 for fluorescence lifetime data for CaRuby-Cl and -F.

Table 2. Fluorescence Lifetimes of CaRuby Dyes[a]

CaRuby	t_f (ps)	t_s (ns)	*S*-factor	$K_{D,Ca}$ (μM)
-Me	217 ± 3	3.66 ± 0.12	0.14 ± 0.01	3.4 ± 0.3
-F	232 ± 2	3.74 ± 0.02	0.09 ± 0.02	(9.4 ± 2.5)
-Cl	160 ± 9	3.61 ± 0.04	0.12 ± 0.01	20.6 ± 4.4

[a]Mean and SD values; n = 3 measurements for each dye.

at 33 °C in CaRuby-Me (1 μM, 15 min) from a stock dissolved in methanol (1:2000 final) or S101 (1 μM in water, 15 min). Parallel controls with SR101 dissolved 1:2000 in methanol excluded a possible solvent effect. During experiments that were performed at room temperature (RT, 20–23 °C) slices were constantly perfused with ACSF at 3 mL/min. Cells located near the slice surface were imaged with 1PEF epifluorescence as described below.

4.3. Fluorimetry, Spectroscopy, and Lifetime Measurements. *4.3.1. Evaluation of Divalent-Cation and pH Sensitivity.* Methods used here have been published elsewhere.[16,17,20] Briefly, stock solutions of the three CaRubies were prepared at 1 mM in DMSO and diluted to final concentrations in a reference buffer containing in mM: 100 KCl, 30 MOPS, pH 7.2. Absorbance spectra were recorded on a double-beam UV/vis spectrophotometer (Varian Cary 300, Agilent, Massy-Palaiseau, France). From the same samples, we recorded fluorescence emission spectra in the 544 to 700nm range on a spectrofluorometer (Jasco, France) housing a Xe-arc lamp. Excitation and emission slit widths were both set to 2.5 nm. All measurements were carried out at RT in quartz cuvettes having 1 cm optical path length (QS-115, Hellma, Müllheim, Germany). Fluorescence quantum yield φ was evaluated relative to that of SR101, φ = 1.0 in absolute ethanol,[43] by integrating the spectral emission of the respective CaRubies and SR101 and applying $\varphi = \varphi_{SR101}(s/s_{SR101})(n_{water}/n_{EtOH})^2$ as a correction[44] for the different refractive indices (n = 1.33 and 1.36 for water and ethanol, respectively, at 535 nm. Here, s is the slope of a plot of the integrated fluorescence vs absorbance (Figure S1, Supporting Information). To avoid self-absorption, we worked with solutions having OD 0.01–0.1. The sequence of measurements was altered between titrations to exclude bleaching or evaporation effects.

4.3.2. 2PEF Excitation Spectra. 2PEF was measured at RT upon excitation with a wavelength-tunable fs-pulsed Ti:Sapphire (MaTai HP, SpectraPhysics-Newport, Santa Clara, CA). The excitation wavelength was scanned at equal excitation power from 750 to 1000 nm and the laser beam focused with a water immersion objective (XLUMPFLN 20XW, NA1.0, Olympus, Hamburg, Germany) into a cuvette containing, in mM, 100 KCl, 30 MOPS at pH 7.2. 2PEF was epi-collected, extracted with a 750DCSPXR dichroic filter and ET605/70 band-pass filter (both from Chroma, Bellows Falls, VT) and was detected on a photon-counting GaAsP PMT module (Hamamatsu, H7421-40MOD). The mean excitation power (maintained constant at 5 mW at all wavelengths) was monitored on a power meter (SpectraPhysics Newport, 407A; 1 s integration time) placed immediately after the sample, on the opposite side of the objective. The laser beam was attenuated using a combination of a rotatable half-wave plate and linear polarizer.

4.3.3. Time-Correlated 2PEF Lifetime Measurements. Fluorescence lifetime (FL) curves were acquired as described previously[19,45] using a time-resolved spectrometer (FluoTime 100, PicoQuant; Berlin, Germany) and a time-correlated single-photon counting (TCSPC) computer board (SPC-730, Becker & Hickl; Berlin, Germany). The excitation source was a mode-locked Ti:sapphire laser (Tsunami, Spectra Physics Newport, Santa Clara, CA). A fast photodiode (TDA 200, PicoQuant, Berlin, Germany) synchronized the photon counting to the excitation pulses (880 nm, 80 MHz). A 650 nm short-pass filter (Chroma, Bellows Falls, VT) and a polarizer set to the magic-angle orientation were placed in the emission path. The instrument response function (IRF) was obtained by recording the hyper-Rayleigh scattering from a colloidal gold suspension (G-1652, Sigma, Seelze, Germany). Stock solutions (1 mM) of the dyes were prepared in methanol. Subsequently, the dyes were diluted 1:100 in buffers containing 10 mM EGTA or 10 mM CaEGTA (Calcium Calibration Buffer Kit #1, Invitrogen), used for reciprocal dilution series (Invitrogen) adjusted to cover the Ca^{2+} range of the dyes. The recorded fluorescence decay curves of each calibration were subjected to a double-exponential iterative reconvolution fit (FluoFit software; PicoQuant, v.4.53) in which the decay time constants were set as global parameters. The fast time constant (τ_f) was assigned to the Ca^{2+}-free (apo-) form of the dye under study, and the slow one (τ_b) was assigned to its Ca^{2+}-bound form. The fractional amplitudes of the decay components resulting from the global fit (α_f and α_b) were the Ca^{2+}-dependent parameters in the calibration equations. Ca^{2+}-insensitive offsets in the decay components, attributable to dye impurities[45]or unresolved lifetime components[46] were negligible and ignored in the calibration. Specifically, offsets for the slow component were absent with all dyes, offsets for the fast component were <5% for CaRuby-F, <3% for CaRuby-Cl and <1% for CaRuby-Me and, in all cases, not significantly different from an accordant distribution around 0%. The S parameter was extracted from the calibration curves as described earlier.[45] Ca^{2+} concentrations were estimated as $Ca^{2+} = K_D S\alpha_b/\alpha_f$ (cf. equation in ref [45]).

4.4. Microscopy. *4.4.1. Total Internal Reflection Fluorescence Microscopy and Photoactivation of CatCh-YFP in Cultured Astrocytes.* Dual-color excitation dual-color emission TIRF microscopy and CatCh photoactivation experiments were performed on a custom microscope described in detail elsewhere.[26] Briefly, the 488 and 568 nm lines of an Ar^+/Kr^+-mixed gas laser (CVI MellesGriot, Voisins Le Bretonneaux, France) were isolated with an acousto-optical tunable filter (AA.Opto-Electronic, Orsay, France), focused in the back-focal plane and directed through the periphery of a high-NA oil-immersion objective (PlanApo TIRFM x60/NA1.45, Olympus, Hamburg, Germany). As a consequence, a collimated beam emerges from the objective at an angle exceeding the critical angle for total

internal reflection. The penetration depth ($1/e^2$ intensity) of the evanescent wave was ~200 nm. Fluorescence was extracted with a custom 488/568 nm dual-band dichroic (AHF Analysentechnik, Tübingen, Germany) and home-built dual-viewer device housing a HQ600LP secondary dichroic, HQ535/50 band-pass (green) and HQ600LP long-pass filter (red) (all from Chroma, Bellows Falls, VT) and detected on an electron-multiplying charge-coupled device camera (QuantEM512SC, Photometrics, Tucson, AZ, 16 μm pixel size). All setup components were controlled with Metamorph (Molecular Devices, Sunnyvale, CA). The 488 nm TIRF excitation beam, 488/568 dual-band dichoric and DF535/50 emission filter were used to search for CatCh-YFP expressing cells, before illumination was switched to 568 nm 1 Hz TIRF imaging for monitoring the CaRuby fluorescence. For the photoactivation of CatCh we used brief (0.5−5 s) flashes of 458 ± 9 nm epi-illumination (13.6 mW/mm^2) from a tunable polychromatic light source (Poly II, TILL Photonics, Gräfelfing, Germany). Ca^{2+} imaging was stopped during photoactivation. Time-lapse fluorescence data was corrected with the prestimulus baseline to account for dye leakage or photobleaching.

TIRFM was also used to monitor ATP-evoked $[Ca^{2+}]_i$ changes in the near-membrane region of cultured astrocytes loaded with the Ca^{2+} indicator Fluo-4, AM ($K_{D,Ca}$ ~345 nM). Cells were incubated in dye-containing extracellular solutions (30 min, RT) and then washed for at least 30 min prior to Ca^{2+} imaging. ATP (300 μM) was applied locally via a double-channel perfusion system, one channel delivering the control buffer and the other the ATP-containing solution. To start the stimulation, the control channel was stopped while switching on the ATP channel at the same time, and the reversed procedure was carried out to terminate the stimulation. The different solutions were delivered through plastic tubings (0.8 mm ID, Tygon, Charny, France) to a multichannel holder (AutoMate Scientific, Berkeley, CA) connected to a small (250 μm ID) silica pipette (WPI, Saratosa, FL, USA) positioned ~200 μm away from the cell. Images were streamed at 20 Hz.

4.4.2. Epifluorescence 1PEF Imaging of Acute Brain Slices. Acute mouse brain slices were imaged on a custom upright microscope fitted for alternate 1PEF wide-field epifluorescence and 2PEF scanning microscopy.[47] For 1PEF epifluorescence, we used a Hg-arc lamp, attenuated and filtered with HQ470/40x and HQ560/80x excitation band-pass filters for EGFP and for CaRuby/SR101, respectively. Fluorescence was extracted with 500DCXR and 600DCXR dichroics, DF535/35 and FF01-654/75-25 emission band-pass filters, respectively, and captured on a Marconi Quantix57 CCD detector (Photometrics, Tucson, AZ, 13 μm pixel size). All filters were from Chroma Technology (Bellow Falls, VT) or Semrock (Rochester, NY). For the images shown in Figure 4, the effective pixel size was 630 nm in the sample plane (XLMPlanFluor, x20/NA0.95, Olympus, Hamburg, Germany).

4.4.3. 2PEF in Vivo Imaging. Two 3 months old (body weight 250 g) male Sprague−Dawley rats were anaesthetized with isoflurane (1−1.5%) in O_2/NO_2 (20%/80%), placed on a heating blanket and maintained in a stereotaxic frame using a custom-made mouth piece Heartbeat and breathing were continuously monitored. A 3 mm diameter craniotomy centered at 2.5 mm from the bregma and 5.5 mm laterally was performed above the right hemisphere, and the dura mater was removed. Throughout the surgery the brain was bathed in external saline (in mM: 125 NaCl, 2.5 KCl, 26 $NaHCO_3$, 1.25 NaH_2PO4, 2$CaCl_2$, 1 $MgCl_2$, and 20 glucose).

For 2PEF imaging, a 10 μL drop of 100 μM CaRuby-Me in saline was deposited on the brain surface. The craniotomy was filled with agarose and sealed with a glass coverslip. 2PEF was monitored on a custom in vivo microscope.[48] Upon 900 nm excitation with a MaiTai fs-pulsed Ti:sapphire laser, 150 μm fields of view were scanned at 10 Hz using a combination of a resonant scanner (CRS-Series, GSI) and a galvanometric scanner (M-Series, GSI). Fluorescence detection was achieved with a digital photomultiplier (H7421-40, Hamamatsu). Coordinates from the sinusoidal resonant scan were linearized before analysis. Recordings were acquired in the upper part of the layers 2/3 and small image z-stacks acquired and maximum-projected.

4.5. Data Analysis and Statistics. Image and spectral data were exported and analyzed with MetaMorph (Molecular Devices, Sunnyvale, CA) and IGOR Pro (Wavemetrics, Lake Oswego, OR). Data are shown as mean ± 1 SD, unless otherwise stated. *N* is the number of independent experiments (e.g., animals, titrations), and *n* is the number of cells or of regions interest (ROIs). The significance of the difference between samples was evaluated by ANOVA and *t*-test with MATLAB (The MathWorks, Natick, MA). *p* values less than 0.05 were considered significant.

■ ASSOCIATED CONTENT

Ⓢ Supporting Information

Six supplementary figures and their legends. Details of synthesis and purification of CaRuby-Cl, CaRuby-F, and CaRuby-Me are given. This material is available free of charge via the Internet at http://pubs.acs.org. Complete NMR and mass spectra files are available from the authors upon request.

■ AUTHOR INFORMATION

Corresponding Author

jean-maurice.mallet@ens.fr

Present Addresses

○Biology Faculty, Kazan Federal University, Kazan, Russia.
□Wolfson Institute, University College London, London, U.K.

Notes

The authors declare no competing financial interest.

■ ACKNOWLEDGMENTS

We thank K. Hérault for astrocyte culture, Prof. Dr. E. Bamberg (MPI für Biophysik, Frankfurt) for the CatCh-YFP plasmid, and Drs. E. Audinat and J. S. Kehoe for comments on early versions of the manuscript. This work was supported by the French Agence National de la Recherche (ANR P3N, nanoFRET^2 grant to A.F., J.M.M., and M.O.) and the European Union (FP6 STRP AUTOSCREEN grant and FP7 ERA-NET Neuron nanosyn grant to M.O.).

■ REFERENCES

(1) Paredes, R. M.; Etzler, J. C.; Watts, L. T.; Zheng, W.; Lechleiter, J. D. *Methods* **2008**, *46*, 143.
(2) Palmer, A. E. *ACS Chem. Biol.* **2009**, *4*, 157.
(3) Tsien, R. Y. *Biochemistry* **1980**, *19*, 2396.
(4) Grynkiewicz, G.; Poenie, M.; Tsien, R. Y. *J. Biol. Chem.* **1985**, *260*, 3440.
(5) Kao, J. P.; Harootunian, A. T.; Tsien, R. Y. *J. Biol. Chem.* **1989**, *264*, 8179.
(6) Thomas, D.; Tovey, S. C.; Collins, T. J.; Bootman, M. D.; Berridge, M. J.; Lipp, P. *Cell Calcium* **2000**, *28*, 213.
(7) Knöpfel, T.; Lin, M. Z.; Levskaya, A.; Tian, L.; Lin, J. Y.; Boyden, E. S. *J. Neurosci.* **2010**, *30*, 14998.
(8) Looger, L. L.; Griesbeck, O. *Curr. Op. Neurobiol.* **2012**, *22*, 18.
(9) Bakayan, A.; Vaquero, C. F.; Picazo, F.; Llopis, J. *PLoS One* **2011**, *6*, e19520.
(10) Bannwarth, M.; Corrêa, I. R.; Sztretye, M.; Pouvreau, S.; Feally, C.; Aebischer, A.; Royer, L.; Rios, E.; Johnsson, K. *ACS Chem. Biol.* **2009**, *4*, 179.
(11) He, H. Z.; Lei, L.; Li, J. L.; Shi, Z. *Synth. Commun.* **2009**, *29*, 2074.
(12) Egawa, T.; Hanaoka, K.; Koide, Y.; Ujita, S.; Takahashi, N.; Ikegaya, Y.; Matsuki, N.; Terai, T.; Ueno, T.; Komatsu, T. *J. Am. Chem. Soc.* **2011**, *133*, 14157.
(13) Zhao, Y.; Araki, S.; Wu, J.; Teramoto, T.; Chang, Y. F.; Nakano, M.; Abdelfattah, A. S.; Fujiwara, M.; Ishihara, T.; Nagai, T. *Science's STKE* **2011**, *333*, 1888.

(14) Kramer, R. H.; Fortin, D. L.; Trauner, D. *Curr. Op. Neurobiol.* **2009**, *19*, 544.
(15) Miesenböck, G. *Ann. Rev. Cell Dev. Biol.* **2011**, *27*, 731.
(16) Gaillard, S.; Yakovlev, A.; Luccardini, C.; Oheim, M.; Feltz, A.; Mallet, J. -M. *Org. Lett.* **2007**, *9*, 2629.
(17) Luccardini, C.; Yakovlev, A. V.; Pasche, M.; Gaillard, S.; Li, D.; Rousseau, F.; Ly, R.; Becherer, U.; Mallet, J.- M.; Feltz, A.; Oheim, M. *Cell Calcium* **2009**, *45*, 275.
(18) Prasuhn, D. E.; Feltz, A.; Blanco-Canosa, J. B.; Susumu, K.; Stewart, M. H.; Mei, B. C.; Yakovlev, A. V.; Loukou, C.; Mallet, J. -M.; Oheim, M.; Medintz, I. L. *ACS Nano* **2010**, *4*, 5487.
(19) Wilms, C. D.; Schmidt, H.; Eilers, J. *Cell Calcium* **2006**, *40*, 73.
(20) Nolan, E. M.; Ryu, J. W.; Jaworski, J.; Feazell, R. P.; Sheng, M.; Lippard, S. J. *J. Am. Chem. Soc.* **2006**, *128*, 15517.
(21) Minta, A.; Kao, J. P.; Tsien, R. Y. *J. Biol. Chem.* **1989**, *264*, 8171.
(22) Martin, V. V.; Beierlein, M.; Morgan, J. L.; Rothe, A.; Gee, K. R. *Cell Calcium* **2004**, *36*, 509.
(23) Rashid, F.; Horobin, R. W. *J. Microsc.* **1991**, *163*, 233.
(24) Rashid, F.; Horobin, R. W.; Williams, M. A. *Histochem. J.* **1991**, *23*, 450.
(25) Kleinlogel, S.; Feldbauer, K.; Dempski, R. E.; Fotis, H.; Wood, P. G.; Bamann, C.; Bamberg, E. *Nat. Neurosci.* **2011**, *14*, 513.
(26) Li, D.; Hérault, K.; Isacoff, E. Y.; Oheim, M.; Ropert, N. *J. Physiol.* **2012**, *590*, 855.
(27) Kafitz, K. W.; Meier, S. D.; Stephan, J.; Rose, C. R. *J. Neurosci. Meth.* **2008**, *169*, 84.
(28) Nimmerjahn, A.; Kirchhoff, F.; Kerr, J. N. D.; Helmchen, F. *Nat. Methods* **2004**, *1*, 31.
(29) Appaix, F.; Girod, S.; Boisseau, S.; Römer, J.; Vial, J.-C.; Albrieux, M.; Maurin, M.; Depaulis, A.; Guillemain, I.; van der Sanden, B. *PLoS One* **2012**, *7*, e35169.
(30) Blab, G. A.; Lommerse, P. H. M.; Cognet, L.; Harms, G. S.; Schmidt, T. *Chem. Phys. Lett.* **2001**, *350*, 71.
(31) Xu, C.; Williams, R. M.; Zipfel, W.; Webb, W. W. *Bioimaging* **1996**, *4*, 198.
(32) Spiess, E.; Bestvater, F.; Heckel Pompey, A.; Toth, K.; Hacker, M.; Stobrawa, G.; Feurer, T.; Wotzlaw, C.; Berchner Pfannschmidt, U.; Porwol, T. *J. Microsc.* **2005**, *217*, 200.
(33) Mütze, J.; Iyer, V.; Macklin, J. J.; Colonell, J.; Karsh, B.; Petrášek, Z.; Schwille, P.; Looger, L. L.; Lavis, L. D.; Harris, T. D. *Biophys. J.* **2012**, *102*, 934.
(34) Rickauer, J. P.; Tank, D. W. *Proc. Natl. Acad. Sci. U.S.A.* **2009**, *106*, 15025.
(35) Shen, Z.; Lu, Z.; Chhatbar, P. Y.; O'Herron, P.; Kara, P. *Nat. Methods* **2012**, *9*, 273.
(36) Oheim, M.; Beaurepaire, E.; Chaigneau, E.; Mertz, J.; Charpak, S. *J. Neurosci. Meth.* **2001**, *111*, 29.
(37) Oheim, M.; Naraghi, M.; Müller, T. H.; Neher, E. *Cell Calcium* **1998**, *24*, 71.
(38) Yasuda, R.; Sabatini, B. L.; Svoboda, K. *Nature neuroscience* **2003**, *6*, 948.
(39) Cahoy, J. D.; Emery, B.; Kaushal, A.; Foo, L. C.; Zamanian, J. L.; Chistopheson, K. S.; Xing, Y.; Lubischer, J. L.; Krieg, P. A.; Krupenko, S. A.; Thompson, W. J.; Barres, B. A. *J. Neurosci.* **2008**, *28*, 264.
(40) Li, D.; Hérault, K.; Oheim, M.; Ropert, N. *Proc. Natl. Acad. Sci. U.S.A.* **2009**, *106*, 21960.
(41) Li, D.; Ropert, N.; Koulakoff, A.; Giaume, C.; Oheim, M. *J. Neurosci.* **2008**, *28*, 7648.
(42) Gong, S.; Zheng, C.; Doughty, M. L.; Losos, K.; Didkovsky, N.; Schambra, U. B.; Nowak, N. J.; Joyner, A.; Leblanc, G.; Hatten, M. E. *Nature* **2003**, *425*, 917.
(43) Karstens, T.; Kobs, K. *J. Phys. Chem.* **1980**, *84*, 1871.
(44) J. N. C. Demas, G. A. *J. Phys. Chem.* **1971**, *75*, 991.
(45) Wilms, C. D.; Eilers, J. *J. Microsc.* **2007**, *225*, 209.
(46) Gersbach, M.; Boiko, D. L.; Niclass, C.; Petersen, C. C. H.; Charbon, E. *Opt. Lett.* **2009**, 34.
(47) Ducros, M.; van't Hoff, M.; Evrard, A.; Seebacher, C.; Schmidt, E. M.; Charpak, S.; Oheim, M. *J. Neurosci. Meth.* **2011**, *198*, 172.
(48) Kremer, Y.; Léger, J.-F; Goodman, D.; Brette, R.; Bourdieu, L. *J. Neurosci.* **2011**, *31*, 10689.